Available online at www.sciencedirect.com
ScienceDirect
International Journal of Heat and Mass Transfer 50 (2007) 4195–4205
International Journal of HEAT and MASS TRANSFER
www.elsevier.com/locate/ijhmt

Oscillatory thermocapillary flow in liquid bridges of high Prandtl number fluid with free surface heat gain

Aihua Wang [a], Yasuhiro Kamotani [a,*], Shinichi Yoda [b]

[a] Department of Mechanical and Aerospace Engineering, Case Western Reserve University, Cleveland, OH 44106, USA
[b] Japan Aerospace Exploration Agency, Tsukuba-shi, Ibaraki 305-8505, Japan

Received 27 August 2006; received in revised form 24 February 2007
Available online 3 May 2007

Abstract

Oscillatory thermocapillary flow in liquid bridges of high Prandtl number fluid is studied. The effect of free surface heat transfer, especially heat gain, on the oscillation phenomenon is investigated experimentally and numerically. It is shown that the critical temperature difference (ΔT_{cr}) changes substantially when the free surface heat transfer changes from loss to gain in the case of nearly straight liquid bridges. In contrast, ΔT_{cr} is not affected by the free surface heat transfer with concave liquid bridges. The free surface heat transfer rate is computed numerically by simulating the interaction of the liquid and the surrounding air. The oscillatory flow is also investigated numerically by analyzing the liquid flow in three-dimensions for straight bridges. The computed results agree well with the experimental data. The simulation shows that the free surface heat gain enhances the surface flow and that the oscillatory flow is a result of interactions between the convection effect and buoyancy. The flow does not become oscillatory if there is no net heat gain at the free surface in the range of Marangoni number of the present work ($\leqslant 1.8 \times 10^4$), so the present cause of oscillations is different from that in the free surface heat loss case we investigated in the past.

Keywords: Thermocapillary flow; Liquid bridge; Oscillations; Buoyancy; Experiment; Simulation

1. Introduction

Much work have been done on oscillatory thermocapillary flow in the half-zone, or liquid bridge, configuration, in which a liquid column is suspended between two differentially heated walls (e.g. [1–3]). It is known that the flow becomes oscillatory for a wide range of Prandtl number (Pr). However, the cause of oscillations for high Pr fluid ($Pr > 20$) is not yet fully understood. One reason for this lack of understanding is that available experimental data are somewhat confusing and contradictory due to various effects, as pointed out in [3]. The shape of the liquid bridge is known to play an important role in oscillatory thermocapillary flow of high Pr fluids (e.g. [3,4]). Buoyancy is not completely negligible in ground-based experiments. Oscillatory buoyant–thermocapillary flow in liquid bridges has been investigated [5] and some experiments were conducted in microgravity (e.g. [6]). In the configuration where the liquid is heated from above, buoyancy tends to stabilize the flow. It has recently been found that the onset of oscillations in high Pr fluids is very sensitive to the heat transfer at the free surface. Heat is lost from the free surface in typical room temperature experiments. The heat loss is associated mainly with natural convection of the surrounding air induced by the heating and cooling arrangement used in the experiment. Under typical conditions, the natural convection is relatively week, so its effect has been neglected in the past. However, Kamotani et al. [7,8] and Shevtsova et al. [9] have shown that the onset of oscillations is very sensitive to the heat loss: the critical temperature difference changes by a factor of two to three when the surrounding air

* Corresponding author.
E-mail address: yxk@case.edu (Y. Kamotani).

0017-9310/$ - see front matter © 2007 Elsevier Ltd. All rights reserved.
doi:10.1016/j.ijheatmasstransfer.2007.02.035

Nomenclature

Ar	liquid bridge aspect ratio, L/D
Bi^*	modified average Biot number over free surface
Bi^*_{loc}	local modified Biot number, $qR_0/(k\Delta T)$
Bo_d	dynamic Bond number, $Gr/R\sigma = \rho g\beta L^2/\sigma_T$
Bo_s	static Bond number, $\rho g L^2/\sigma$
D	diameter of liquid bridge base
D_0	diameter of liquid bridge neck (see Fig. 1)
Dr	diameter ratio, D_0/D
g	gravitational acceleration
Gr	Grashof number, $g\beta\Delta TL^3/\nu^2$
k	thermal conductivity
L	liquid bridge height
Ma	Marangoni number, $\sigma_T\Delta TL/\mu\alpha$
Ma_{cr}	critical Ma for onset of oscillations
Pr	Prandtl number, ν/α
q	local heat transfer rate at free surface
R_0	radius of liquid bridge base
$R\sigma$	surface tension Reynolds number, Ma/Pr
T	temperature
T_C	cold wall temperature
T_H	hot wall temperature
T_R	ambient air temperature
$\overline{T}$	azimuthally averaged temperature defined in Eq. (1)
T'	disturbance temperature, $T - \overline{T}$
u	velocity component in z direction
(r, z)	coordinates for liquid flow defined in Fig. 1
(R, Z)	global coordinates defined in Fig. 2

Greek symbols

α	thermal diffusivity
β	coefficient of thermal expansion
ΔT	imposed temperature difference, $T_H - T_C$
ΔT_{cr}	critical temperature difference
θ	azimuthal coordinate
μ	dynamic viscosity
ν	kinematic viscosity
ρ	density
σ	surface tension
σ_T	temperature coefficient of surface tension
ψ	stream function in cylindrical coordinates

temperature is varied. Therefore, we have to take this sensitivity into account when we explain the oscillation mechanism for high Pr fluid. Since this heat loss experiment gave us significant insight into the oscillatory thermocapillary flow, we have extended the work to include free surface heat gain. Our earlier results [8] indicated there is a difference between the cause of oscillations with heat loss and that with heat gain.

In addition to the experiment, three-dimensional numerical simulation of the oscillatory flow is performed. Oscillatory thermocapillary flows in liquid bridges have been simulated in the past for various Pr fluids (e.g. [10–13]). Sim and Zebib [14] investigated the effect of heat loss on the instability. However, oscillatory buoyant–thermocapillary flow with free surface heat gain has never been simulated in the past. The present simulation shows that the experimentally observed oscillations with free surface heat gain are induced by the interaction between thermocapillarity and buoyancy. The free surface heat gain makes the flow active over a wider region, which makes it easier for the flow to become oscillatory.

Because of the fact that there is some work to be done in order to fully the understand oscillatory thermocapillary flows of high Prandtl fluids, JAXA (Japan Space Exploration Agency) organized a research group to conduct a comprehensive study of the subject. The group is preparing a microgravity experiment to be conducted aboard the Space Station in the near future. The present work is done in conjunction with this effort. The present paper is based partially on the thesis by Wang [15].

2. Experimental work

The liquid bridge configuration is illustrated in Fig. 1. The experimental setup is similar to the ones used and described in our various earlier experiments ([3,7,8,15]). The top and bottom rods are made of copper. Two and 3 mm rods are used in the present work. The rod temperatures are monitored by inserted thermocouples. Two and 5-centistokes (cSt) silicone oils are used as the test fluid. The bottom rod is cooled by cooling water from a constant temperature bath. The main difference from our earlier systems is the top rod. The top rod was heated by a nichrome wire in our past experiments. In the present experiment with heat gain, in which the ambient temperature is kept above the hot wall temperature, the top wall must be

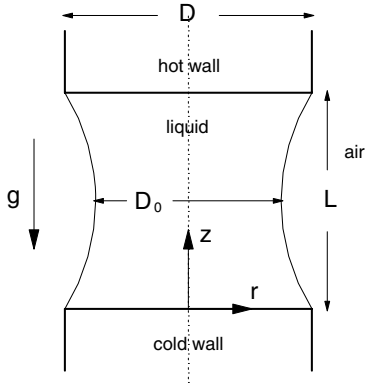

Fig. 1. Liquid bridge configuration.

cooled, so the top rod was cooled by water from a constant temperature bath. The apparatus is placed in an oven to vary the surrounding air temperature. The flow is visualized by adding a small amount of alumina particles (about 10–20 μm in diameter) to the test fluid. The fluid motion is observed by a video camera which is attached to a microscope.

The effects of the oven conditions on the flow are discussed in [8]. Although there is a weak air motion in the oven and the oven temperature changes with time and location to a certain degree, its effect on the flow and on the onset of oscillations has been judged to be negligible. Pertinent information to the present work is that at any given time and at any temperature setting, the oven air in the vicinity of the liquid bridge is uniform within ±1 °C. The liquid bridge shape is adjusted to a desired shape after the oven temperature is stabilized.

The rod temperatures are measured with 0.1 °C accuracy. The liquid column length and shape are kept within ±2% of the specified values. The error in the measurement of the critical temperature difference is estimated to be within 5%. The properties of the test fluids are given in [16].

3. Important parameters

The basic dimensionless parameters for the steady thermocapillary flow in the present configuration are known to be Ma (Marangoni number), Pr, and Ar (aspect ratio). The effect of buoyancy on the flow is represented by Bo_d (dynamic Bond number). Bo_d is the ratio of Grashof number (Gr) of natural convection to the surface tension Reynolds number ($R\sigma = Ma/Pr$) of thermocapillary flow, $Bo_d = Gr/R\sigma$. The effect of gravity on the liquid column shape is represented by Bo_s (static Bond number). It is known that the onset of oscillations is quite sensitive to the column shape. The shape is adjusted by adjusting the total volume of the liquid. As in our past work, the shape is represented by Dr (diameter ratio). Although our main interest is straight liquid bridges (Dr = 1), some tests are also conducted with concave bridges (Dr < 1).

Another important parameter is associated with the heat transfer at the free surface. One can quantify the local heat transfer rate by the heat transfer coefficient and the difference between the free surface and ambient temperatures, so we need two dimensionless parameters. Since the liquid bridge is rather small in the present work, it is very difficult to experimentally determine the free surface heat transfer rate accurately. Therefore, as was done in our past work, we compute it based on the numerical simulation, as will be discussed later. Since we compute the heat transfer rate (q) in this situation and since q itself is the main quantity of interest in the present work, we represent the heat transfer by the dimensionless q, namely Bi^*_{loc} (modified local Biot number), instead of using two parameters, as discussed in detail in [8]. The average value of Bi^*_{loc} over the entire free surface is Bi^* (modified average Biot number). Using the same convention as in out past work, Bi^*_{loc} is positive when heat is lost from the surface and negative for heat gain.

The parametric ranges of the present work with free surface heat gain are: Ar = 0.7 for $D = 2$ mm ($L = 1.4$ mm) and 0.67 for $D = 3$ mm ($L = 2$ mm), Pr = 27–30, and $Ma = 1 \times 10^4$–1.8×10^4. In some heat loss tests, Ma goes up to 5×10^4. The fluid viscosity is evaluated at the fluid mean temperature, 1/2 ($T_H + T_C$). Dr ranges from 0.55 to 1. Bo_d is equal to 0.6 for $D = 3$ mm and 0.27 for $D = 2$ mm. The static Bond number, Bo_s, is 0.9 for $D = 2$ mm and 1.8 for $D = 3$ mm. The liquid bridge is not exactly straight for Dr = 1 in this Bo_s range. However, as we discussed in [3], the liquid radius variation is only ±2% even at $Bo_s = 2$, so the flow is not much affected by this shape change. Bi^* ranges from −0.5 (gain) to 0.4 (loss). It can be shown that the ratio of the total heat loss from the free surface to the total heat transfer through the liquid is given by $4\mathrm{Ar}Bi^*/Nu$, where Nu (Nusselt number) is the ratio of convection to conduction heat transfer through the liquid. The ratio is less than 0.2 in the present work, so the heat loss from the free surface is relatively small.

4. Numerical simulation

In conjunction with the experimental work we perform numerical simulations for two purposes. One purpose is to compute the free surface heat transfer rate and the other is to study the oscillation mechanism. We use an axisymmetric model for the former purpose and a 3-D model for the latter.

The two-dimensional model has been used in our heat loss work and described in detail in [8]. It is based on SIMPLER [17] to investigate steady flow and heat transfer. The computational domain includes the liquid bridge, the surrounding air, and the hot and cold rods, as illustrated in Fig. 2. Cylindrical coordinates (r, z) are used for the liquid flow analysis (Fig. 1), and for the air flow analysis, the global coordinates (R, Z) are used (Fig. 2). The liquid axial velocity is non-dimensionalized by $\sigma_T \Delta T/\mu(R/L)$. The liquid temperature is made dimensionless as $(T - T_C)/\Delta T$.

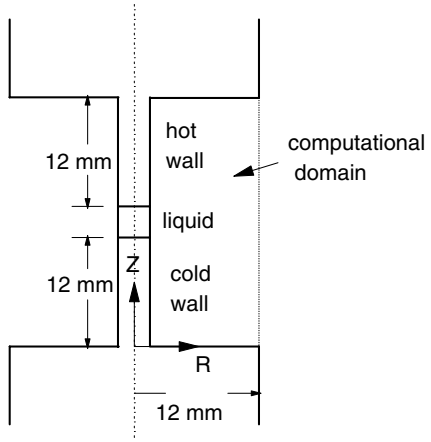

Fig. 2. Computational domain for free surface heat transfer calculation.

Based on the grid-dependency study conducted in our earlier work, we use a 51×58 ($r \times z$) grid for the liquid domain with the smallest dimensionless axial mesh size next to the hot and cold walls being 0.001. For the air domain, we use a 51×159 ($R \times Z$) grid with the smallest radial mesh next to the liquid being 0.0005. Using this grid, the predicted temperature distributions in the air have been shown to agree well with the experimental data [8]. Therefore, for given experimental conditions we use this program to compute the free surface heat transfer rate. The program includes radiation heat transfer with the surface emissivity equal to 0.9 [18]. The radiation contribution is found to be less than 15%.

In the present work, we compute the heat transfer rate also for curved free surfaces. In this case we employ the code based on a boundary-fitted coordinate system that we developed in the past [19]. For a given Bo_s, Dr, and Ar, we compute the static free surface shape first by solving the static meniscus equation [3]. Then, the coordinate system for flow analysis is setup based on this free surface shape. This procedure is justified because the free surface deformation caused by the flow itself is very small, less than 0.1%, as the capillary number of the flow is smaller than unity, on the order of 0.03 [3]. The same grid as used in the straight free surface shape is used.

The above straight free surface code is extended to 3-D for oscillatory flow study since the oscillatory flow is observed to be generally non-axisymmetric. Under the present experimental conditions, the natural convection of the surrounding air is induced mainly by the heating and cooling arrangement of the experiment. Although the liquid motion induces air motion by the shear at the interface, its contribution to the surface heat transfer is much smaller than the buoyancy driven flow [3]. Therefore, for given conditions the heat transfer rate is virtually unchanged whether the liquid flow is steady or oscillatory as long as the oscillation level is not very high. Since our interest in the present work is the oscillatory flow near the onset where the oscillation level is low, we calculate the surface heat transfer, for given conditions, based on the axisymmetric flow model and use this information in the 3-D calculation for the same conditions. In this way we do not have to simulate the air flow in the 3-D oscillatory flow study.

In a 3-D calculation we start with an axisymmetric solution, but the flow gradually loses the symmetry and becomes time-oscillatory. Eventually the oscillation amplitude becomes constant, which is the state of interest. The effect of the numerical grid on the oscillation amplitude is investigated. It is found that it is important to have a sufficiently small grid next to the free surface in order to obtain an oscillatory flow with free surface heat gain. As in the axisymmetric calculation a 51×58 ($r \times z$) grid is used with the smallest radial mesh size next to the free surface being equal to 0.0004. A uniform grid is used in the azimuthal direction. Appropriate mesh size in the azimuthal direction is chosen by investigating its effect on the oscillatory flow. Three different numbers of grid are tested, namely 17, 29, and 41. For the conditions of $Ma = 1.5 \times 10^4$, $Pr = 28$, $\mathrm{Ar} = 0.67$, $\mathrm{Dr} = 1$, and $Bi^* = -0.24$ (heat gain), the flow becomes oscillatory with all of the grids, and they all show nearly identical oscillatory flow structure. The oscillation frequency and the temperature oscillation level at the free surface at the mid-height of the liquid column are nearly identical (within 3%) with those grids. Therefore, 29 meshes are used in the azimuthal direction.

5. Results and discussion

5.1. Experimental data

In most of the tests the cold wall temperature (T_C) is maintained at around 22 °C. After we set T_R at a desired level, we increase T_H incrementally until the flow transitions to oscillatory flow, judged by the flow observation. The oscillatory flow structure in the case of free surface heat loss (usually room temperature tests) has been described in the past (e.g. [1]). During oscillations, the flow is relatively active near the hot wall, since the flow is mainly driven in the region called the hot corner. The oscillatory flow with heat gain is generally similar to the flow with heat loss. In the parametric range of the present experiment, the flow structure is of rotating-type with the azimuthal wave number equal to one ($m = 1$ mode), but sometimes we observe a pulsating pattern of $m = 1$ especially when the oscillation level is very weak. The oscillatory flow with gain is more active in the bulk region than the flow with heat loss [15].

The temperature difference across the liquid bridge at the onset of oscillations is called the critical temperature difference (ΔT_{cr}). The values of ΔT_{cr} measured under various conditions are presented in Fig. 3. The abscissa of the figure is $T_R - T_C$. In room temperature tests, $T_R \approx T_C$ and it is a heat loss situation as $T_H > T_R$. The situation changes from heat loss to gain with increasing ($T_R - T_C$). As Fig. 3

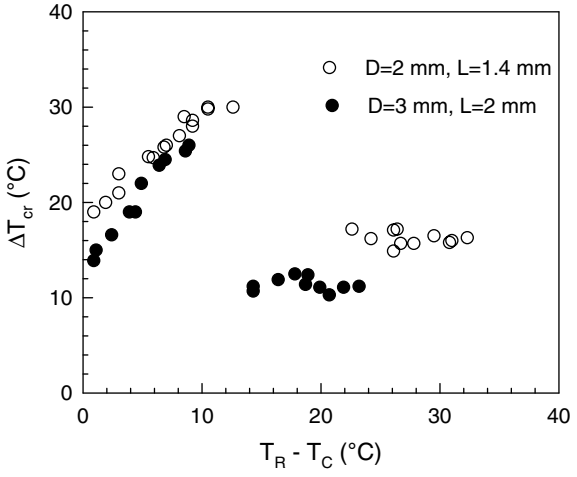

Fig. 3. Critical temperature difference vs. ambient temperature.

shows ΔT_{cr} suddenly drops beyond a certain $(T_R - T_C)$. When $(T_R - T_C)$ is below this value, ΔT_{cr} is very sensitive to the ambient temperature. This trend with heat loss has been investigated earlier [8]. Apparently, around the situation when the heat transfer changes from loss to gain, something happens.

In order to determine whether we have heat gain or loss, we compute Bi^* from the numerical simulations based on the experimental data. ΔT_{cr} is non-dimensionalized as Ma_{cr} (critical Marangoni number). The result is shown in Fig. 4. It is clear that there are two different trends: one for heat loss (positive Bi^*) and one for heat gain (negative Bi^*). While Ma_{cr} is extremely sensitive to Bi^* with heat loss, it is not significantly affected by Bi^* with heat gain. The data shows that the flow with heat gain becomes oscillatory beyond Ma of about 1.4×10^4.

The oscillation frequency is not investigated systematically in the present work. For later comparison, the oscillation period is approximately 1.2 s for $D = 3$ mm at $Ma = 1.5 \times 10^4$ [15]. The frequency is not a strong function of Bi^* at a given Ma.

It is known from past room temperature tests that the onset of oscillations is a strong function of Dr [3]. For a given Ar, a plot of Ma_{cr} against Dr shows two distinct trends: one for Dr near unity, called the fat branch, where Ma_{cr} increases sharply with decreasing Dr and one branch for smaller Dr, called the slender branch, where Ma_{cr} is a much weaker function of Dr. For Ar near 0.7 in the present experiment, the dividing Dr is known to be about 0.8. Since the results in Figs. 3 and 4 represent the fat branch, we investigate the slender branch in Fig. 5, where ΔT_{cr} is plotted vs. $(T_R - T_C)$ for nearly fixed Dr (=0.6–0.7). As the figure shows, ΔT_{cr} is not much affected by $(T_R - T_C)$, which is quite a contrast to the trend in the fat branch (Fig. 3). Based on the data in Fig. 5, Ma_{cr} and Bi^* are computed, which are plotted in Fig. 6. The figure shows that in the parametric range of the present experiment, Ma_{cr} is not affected appreciably by Bi^*, whether we have heat gain or loss.

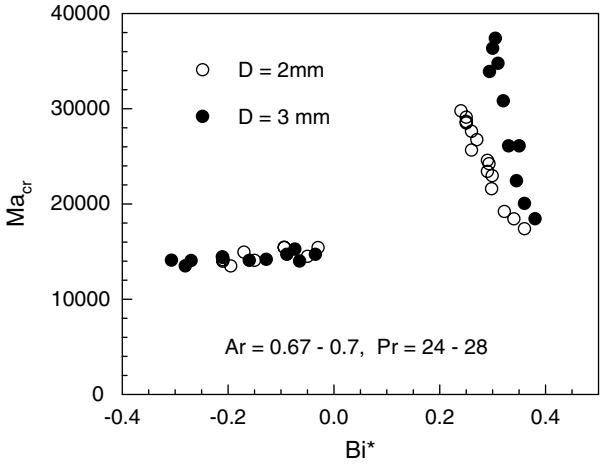

Fig. 4. Critical Marangoni number vs. modified average Biot number.

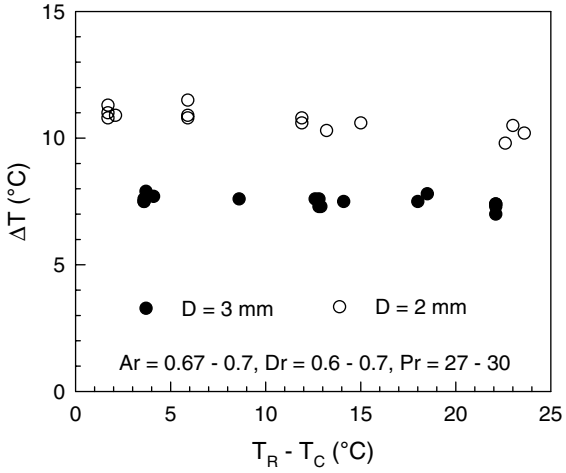

Fig. 5. Critical temperature difference vs. ambient temperature for concave liquid bridge.

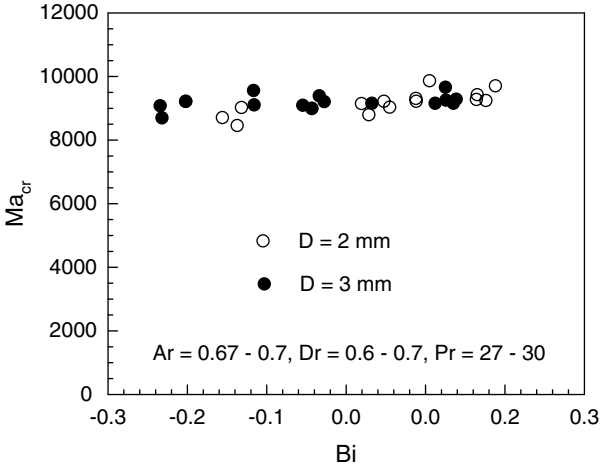

Fig. 6. Critical Marangoni number vs. modified average Biot number for concave liquid bridge.

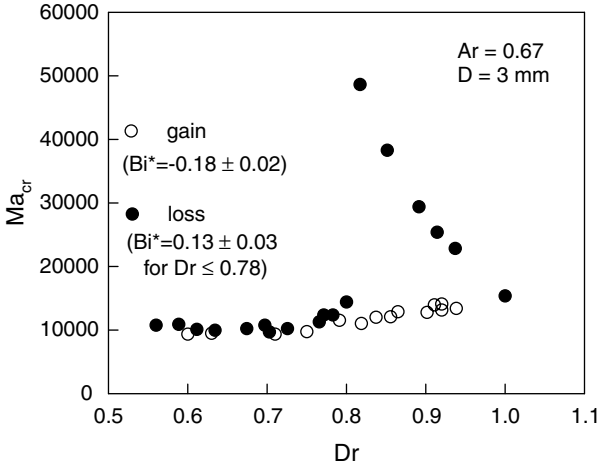

Fig. 7. Critical Marangoni number vs. liquid bridge shape for heat gain and loss cases.

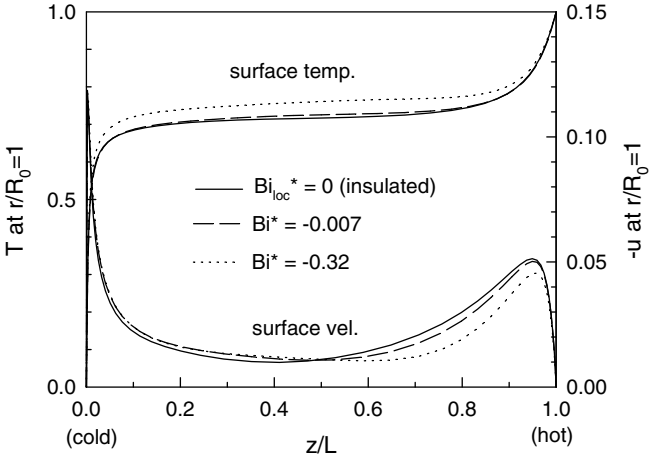

Fig. 8. Effect of heat gain on free surface velocity and temperature distributions ($Ma = 1.4 \times 10^4$, Ar = 0.7, $Pr = 28$, and $Bo_d = 0.27$).

Fig. 7 shows how Ma_{cr} varies with Dr for nearly fixed Bi^*. Although Ma_{cr} is not affected by Bi^* below Dr of about 0.8, it increases sharply beyond Dr of about 0.8 with heat loss (positive Bi^*), which is well known. In contrast, Ma_{cr} changes very gradually with Dr with heat gain. We do not see a jump in Ma_{cr} even near Dr of unity (straight bridge) with heat gain.

Judging by the data shown above, it appears that the oscillatory flow with heat gain is fundamentally different from that with heat loss. The numerical analysis is conducted to clarify the difference.

5.2. Numerical results: basic flow

Before we study the oscillatory flow, it is useful to know the basic flow field with free surface heat gain. Since the main driving force is related directly to the temperature distribution along the free surface, Fig. 8 shows how the surface temperature and velocity distributions are affected by the overall heat transfer rate (Bi^*). When the free surface is insulated ($Bi^*_{loc} = 0$), a large surface temperature gradient exists near the hot wall, which makes the flow active in the hot corner. With increasing heat gain, the temperature gradient in the hot corner decreases but increases in the bulk region.

This effect of heat gain on the flow can be seen more clearly in the streamline patterns shown in Fig. 9. The streamlines are contours of constant stream function (ψ). The maximum stream function, ψ_{max}, represents the overall strength of the flow, especially near the hot wall. The values of ψ_{max} are also given in Fig. 9. ψ_{max} is non-dimensionalized by $\sigma_T \Delta T/\mu(R^3/L)$. As the figure shows, the liquid motion is mainly centered near the hot wall with the insulated surface, but the cell center is more elongated towards the cold wall with heat gain. As discussed above, the flow is experimentally observed to be more active in the bulk region with heat gain. Although the hot corner is less active with heat gain (ψ_{max} decreases with heat gain), ψ_{max} still occurs near the hot wall, so the region near the hot wall remains important for the flow. The flow along the free surface towards the cold wall is called the surface flow, and the interior flow towards the hot wall is called the return flow herein.

Typical local Biot number distributions are shown in Fig. 10 for heat gain and loss cases. In both cases there is a small region of large heat loss near the cold wall as the liquid is cooled by the cold wall through the air. This heat loss increases the surface temperature gradient near the cold wall and thus activates the flow in this region. Otherwise, the heat transfer rate is relatively uniform over a large part of the surface. Although we need to use Bi^*_{loc} to

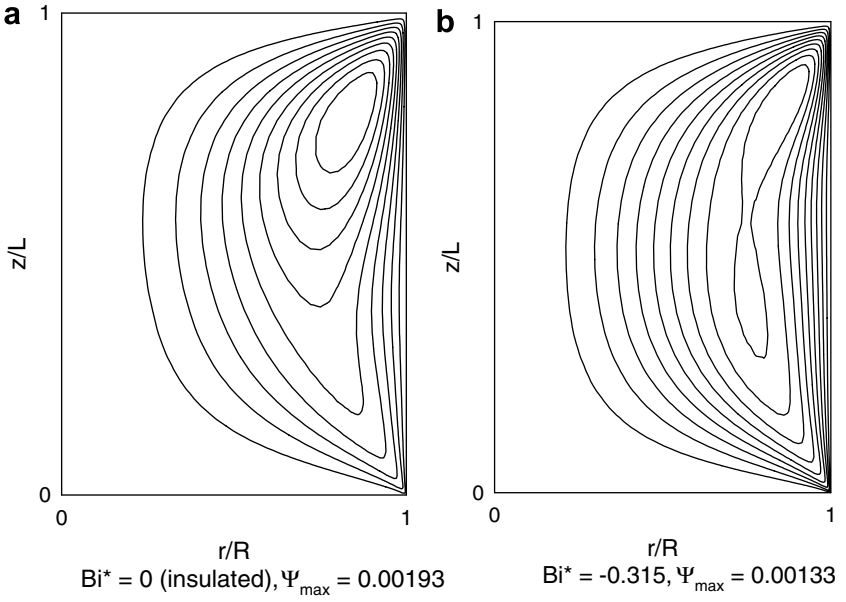

Fig. 9. Effect of heat gain on streamline patterns ($Ma = 1.4 \times 10^4$, Ar = 0.7, $Pr = 28$, and $D = 2$ mm).

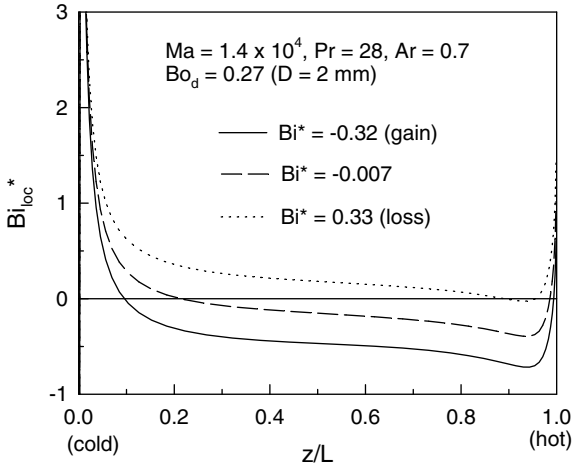

Fig. 10. Local modified Biot number distribution.

represent the surface heat transfer accurately, Bi^*_{loc} has nearly similar distribution, so we use just Bi^* to represent the heat transfer in the present work, for simplicity. Note that even when $Bi^* \approx 0$ ($Bi^* = -0.007$ in Fig. 10), there are regions of appreciable heat gain and loss, as seen in Fig. 10, so it is different from the insulated surface case in which $Bi^*_{loc} = 0$ everywhere.

As discussed in [20], one important feature of thermocapillary flow of high Pr fluid is that the flow is viscous-dominated even when the Reynolds number is much larger than unity because the flow is driven in a relatively small region near the hot wall. This remains true in the present work with heat gain. The effect of inertia forces can be assessed by eliminating the inertia terms in the program (only in the liquid flow). For example, at $Ma = 1.5 \times 10^4$ and $Pr = 28.5$ ($R\sigma = 526$), ψ_{max} decreases 6% if we eliminate the inertia terms in the case of insulated free surface. At the same $R\sigma$ but with $Bi^* = -0.24$, ψ_{max} decreases only 2%. Therefore, the inertia forces do not affect the basic flow significantly in the present parametric range.

The effect of buoyancy on the flow can be assessed in the same way, by eliminating the buoyancy term in the liquid flow. In the present configuration, buoyancy opposes the thermocapillary driving force. Since Bo_d is not much less than unity in the present work (0.6 and 0.27 for $D = 3$ and 2 mm, respectively), we expect some effect from buoyancy. For example, at $Ma = 1.5 \times 10^4$ and $Bi^* \approx -0.24$, the increases in ψ_{max}, if we eliminate buoyancy, are 8% and 4% for $Bo_d = 0.6$ and 0.27, respectively. However, since ψ_{max} occurs in the region where the effect of thermocapillarity is relatively strong, one expects a larger effect of buoyancy away from the hot wall and away from the free surface. In this regard, buoyancy becomes more important with increasing heat gain as the flow becomes more active over a wider area. As will be discussed later, the flow will not become oscillatory without buoyancy and heat gain in the present parametric range.

5.3. Numerical results: oscillatory flow

Although the experimental results suggest that the oscillatory flow with heat gain is different from that with heat loss, we need additional information to identify the cause of oscillations with heat gain. The numerical analysis is performed for this reason. The analysis is done only for the straight liquid bridge case. With insulated free surface, Ma_{cr} is about 4×10^4 [8], so it is difficult to numerically analyze the 3-D oscillatory flow accurately due to the existence of very thin hot corner [20]. Since Ma_{cr} is found to be as small as 1.2×10^4 with heat gain, the numerical simulation can be performed more accurately in the present case.

It is found that the flow does not become oscillatory in the present parametric range unless buoyancy is included in

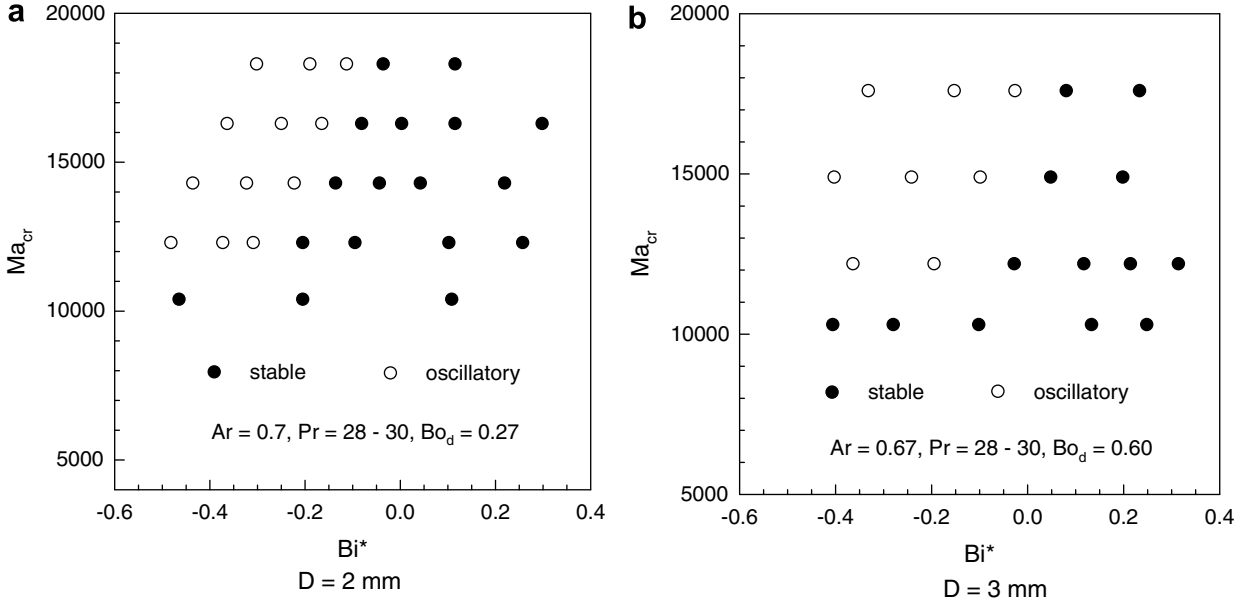

Fig. 11. Flow maps showing oscillatory and steady regimes.

the liquid flow. This means that we can expect some differences between the 2 and 3 mm diameter cases. The flow maps for the two cases are given in Fig. 11. The map shows whether the flow is steady or oscillatory for various conditions. No attempt is made in the present work to identify Ma_{cr} exactly. Fig. 11 shows that the flow becomes oscillatory mainly when we have heat gain (negative Bi^*), in agreement with the experimental observation. Comparing Figs. 11a and b, one sees that, for a given Ma, the flow for $D = 3$ mm becomes oscillatory with smaller heat gain than the flow with $D = 2$ mm. There is also a minimum Ma below which no oscillatory flow exists even with heat gain. The minimum Ma is about 1.1×10^4. Experimentally the hot wall temperature is always maintained below the surrounding air temperature in a heat gain test. At the beginning the heat gain is relatively large. As T_H is increased gradually, Ma increases while the heat gain decreases (Bi^* increases). Normally we still have sufficient heat gain when Ma reaches the minimum critical value. In this situation the flow becomes oscillatory when Ma reaches the minimum critical value, independent of Bi^* at that time. This is the trend we observe experimentally (Fig. 4), although the minimum Ma is about 1.4×10^4.

Fig. 4 shows that the flow becomes oscillatory in the present range of Ma when the heat loss is large enough. In fact, in our previous work with heat loss [8] it was shown that Ma_{cr} becomes as small as 7×10^3 when Bi^* is made large enough (Bi^* about 0.7). However, the present analysis shows that, in the range of Ma investigated herein, the flow remains stable even when Bi^* is increased up to about 0.7. With increasing heat loss, the main driving force becomes more confined to a small region next to the hot wall. Then, as the wall effect becomes increasing large, the flow becomes increasingly viscous-dominated [20]. It is also known that the flow with heat loss becomes oscillatory even in microgravity. These facts suggest that the oscillatory flow in the heat loss regime, including the insulated free surface condition, is fundamentally different from the present flow with heat gain. We have concluded in our earlier work that it is not possible to explain the cause of the oscillatory flow with heat loss observed around $Ma_{cr} \approx 10^4$ simply by the weak inertia forces. We must consider an additional feature to explain the oscillation mechanism with heat loss [8], but the cause of the oscillatory flow with heat gain is simpler.

Typical free surface temperature variations during oscillations at four points, equally spaced circumferentially, at the liquid mid-height are presented in Fig. 12. The figure shows that the oscillatory flow has one temperature peak and one valley in the azimuthal direction ($m = 1$) and is pulsating (non-rotating). The oscillation period in Fig. 12 is 1.2 s, which is in good agreement with the aforementioned experimentally observed period. As discussed earlier, the observed oscillatory flow structure is mainly of rotating-type, although sometimes we observe the pulsating pattern computed above. We tend to observe the pulsating pattern near the onset of oscillations. The differences between the experimental and numerical results will be discussed later.

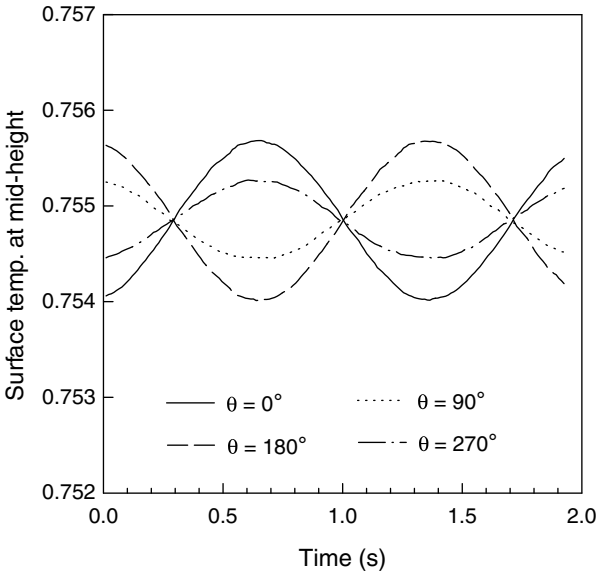

Fig. 12. Free surface temperature variations with time at mid-height during oscillations ($Ma = 1.5 \times 10^4$, Ar = 0.67, $Pr = 29$, and $Bo_d = 0.6$ ($D = 3$ mm)).

In order to show the oscillatory flow structure in more detail, the disturbance temperature field is computed. First, we compute the azimuthally averaged temperature field, namely

$$\overline{T}(r,z) = \frac{1}{2\pi}\int_0^{2\pi} T(r,\theta,z)\,\mathrm{d}\theta. \tag{1}$$

The disturbance temperature is defined as $T'(r,\theta,z) = T(r,\theta,z) - \overline{T}(r,z)$. Note that all temperatures are dimensionless.

The contours of constant T' in the cross-section at mid-height are shown in Fig. 13 at a certain time during oscillations. The figure shows the fluid is relatively warm in half of the cross-section and cold in the other half at this time. These hot and cold spots exist in the return flow region. During oscillations these hot and cold spots become alternately strong and weak. Since the flow is pulsating, there exists a fixed meridional plane where the disturbance amplitude is largest. The contours of constant T' in this meridional plane are shown in Fig. 14 at various times during oscillations. As seen in the figure, the hot and cold spots move with the return flow. Experimentally, the surface flow in a given meridional plane is observed to alternately accelerate and decelerate in one cycle of oscillations. We call these periods the active and weak periods, respectively. In the numerical work, we use the surface velocity at the mid-height to represent the surface flow activity. The computed surface velocities at the mid-height are shown in Fig. 15 in the plane where the disturbance is largest. The times corresponding to Fig. 14 are identified in the figure.

It is found that the flow becomes oscillatory even if we eliminate the inertia terms, with only small changes in the

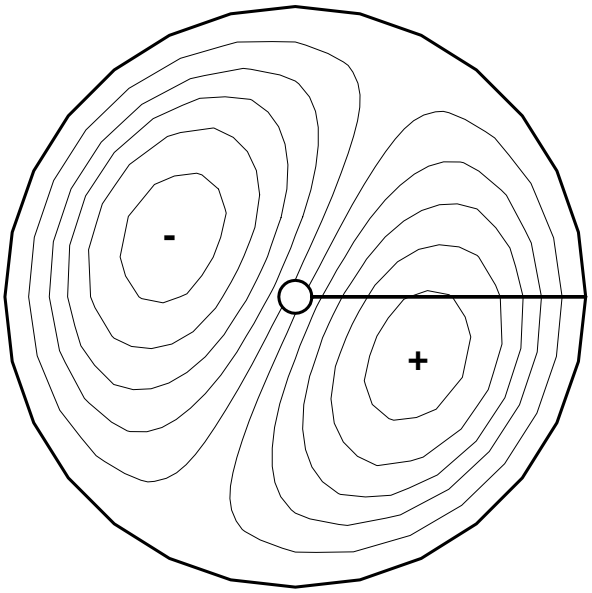

Fig. 13. Contours of constant disturbance temperature in cross-section at mid-height ($Ma = 1.5 \times 10^4$, Ar = 0.67, $Pr = 29$, and $Bo_d = 0.6$ ($D = 3$ mm)). The contours are equally spaced from the maximum value of 0.0185 to the minimum value of −0.0185.

oscillation frequency and amplitude compared to those with the inertia forces. On the other hand, the flow does not become oscillatory, in the present parametric range, if we eliminate the buoyancy term in the numerical program. However, without buoyancy the initial disturbance is found to decay in an oscillatory manner, with or without the inertia terms. Apparently, buoyancy is augmenting this basic oscillatory behavior for sustained oscillations. As discussed earlier, convection heat transfer is important in the oscillation mechanism since the flow does not become oscillatory below a certain Ma. This means that the flow and temperature fields interact in a non-linear manner during oscillations through the convection effect as well as the

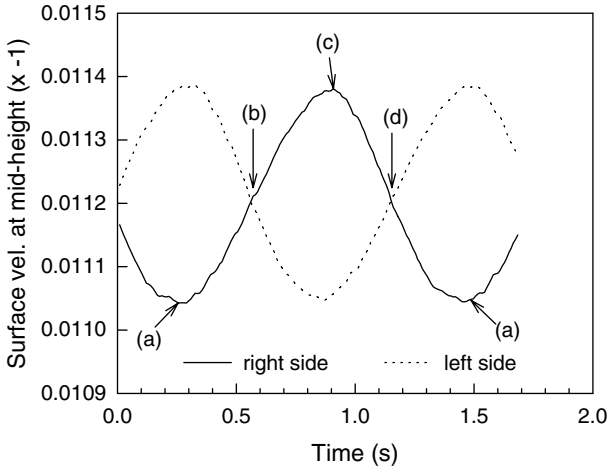

Fig. 15. Surface velocity variations with time in the meridional plane of Fig. 14.

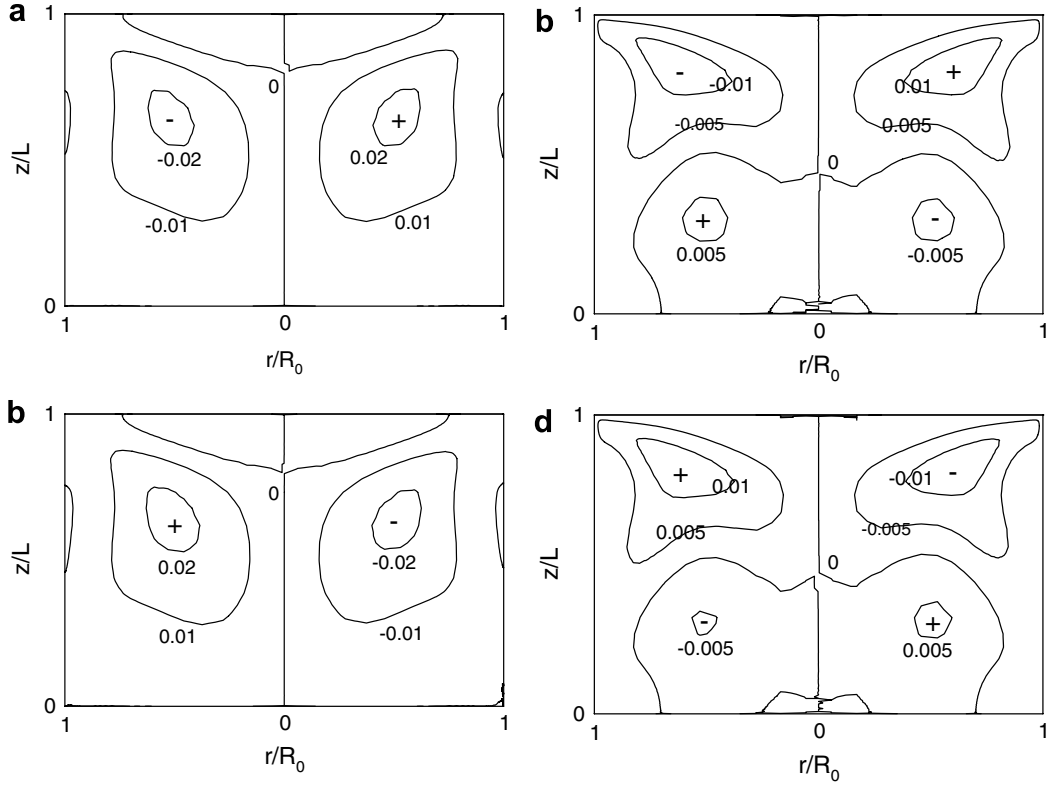

Fig. 14. Disturbance temperature field variation with time in meridional plane where disturbance amplitude is largest ($Ma = 1.5 \times 10^4$, Ar = 0.67, $Pr = 29$, and $Bo_d = 0.6$ ($D = 3$ mm)).

thermocapillarity. This interaction is the cause of the basic oscillatory behavior. Knowing all these facts the oscillation process can be explained as follows.

We focus on the development in the right half of Fig. 14 in the following discussion. In the active period, which is from a to c in Figs. 14 and 15, the hot corner becomes warmer at first as the interior hot spot arrives there (from a to b), which activates the surface flow as the surface temperature gradient increases. Since the interior fluid is warmer, buoyancy also helps to activate the flow. Subsequently, the flow near the cold wall becomes active. As the heat transfer at the cold wall increases, the return flow becomes colder (from b to c). The cold spot near the cold wall also increases the surface temperature gradient, so the surface velocity keeps increasing from b to c. Since the interior fluid is colder, buoyancy now opposes the flow, which eventually makes the region near the cold wall less active. As the cold spot begins to cool the hot corner, the hot corner narrows and the flow also becomes weaker near the hot wall. This is the beginning of a weak period, which is from c to a in Figs. 14 and 15. The weak surface flow eventually makes the bulk fluid becomes warmer again (in the process just opposite to the one in the active period), and the next active period starts.

It is found that if the free surface is thermally insulated, the flow will not oscillate even at the largest Ma of the present study ($=1.8 \times 10^4$). Although the flow does become oscillatory at $Ma = 1.8 \times 10^4$ with $Bi^* \approx 0$, as can be seen in Fig. 11b, there is a region of heat gain over a large portion of the free surface even when Bi^* is nearly zero, as discussed earlier. This shows that the oscillation phenomenon investigated herein requires the free surface heat gain. The role of the heat gain is to make the surface flow active over a wider region, which makes the interaction between the hot and cold corners stronger, an important ingredient in the above oscillation mechanism.

As can be seen in Figs. 12–15, the disturbance amplitude is rather small. In fact, the mean velocity and temperature fields hardly change with time during oscillations. This is true even at high Ma ($\leqslant 1.8 \times 10^4$). Experimentally we determine the onset of oscillations when the flow field is observed to change with time. This explains why the experimentally determined Ma_{cr} ($\approx 1.4 \times 10^4$) is greater than the computed one ($\approx 1.1 \times 10^4$) with heat gain. The oscillation level is observed to increase with increasing ΔT experimentally after the onset of oscillations, but computationally the oscillation level does not increase as much. The fact that oscillation level remains relatively low in the analysis seems to be related to the lack of dynamic interaction between the liquid and the surrounding air, as discussed below.

As discussed earlier, we do not consider the air–liquid interaction during oscillations in the analysis. This is justified when the oscillations level is small. As the oscillation level increases with ΔT, it appears that the liquid and the surrounding air interact dynamically. Notice in Fig. 10 that there is a small region of heat loss near the hot wall regardless of the sign of Bi^*. This occurs because the air coming down along the heater is cooled, just before it gets in contact with the liquid, by the generally cooler air in front of it by conduction. As a result, in the region closest to the hot wall where the liquid temperature is near T_H, the air becomes cooler than the liquid, resulting in heat loss. Although this heat loss region is small, the oscillation phenomenon is very much affected by what happens in the relatively small hot corner, as discussed above. For example, in the beginning of an active period, as the surface velocity increases in the hot corner and more warm air is drawn into this region, the heat loss near the hot wall decreases, which activates the surface flow further and thus aides the oscillation process. This interaction may also explain the difference in the oscillation mode (mainly rotating pattern experimentally and pulsating pattern numerically). The analysis of the oscillation phenomenon including the dynamic interaction with the surrounding air is left for future work.

6. Conclusions

The oscillation phenomenon in liquid bridges of high Prandtl number fluid is investigated experimentally and numerically. It is shown that the heat transfer at the free surface plays an important role in the oscillation mechanism in the case of nearly straight circular bridges. When heat is gained at the free surface, which is the main subject of the present paper, the thermocapillary driving force becomes important over a wider area of the free surface compared to the case of insulated free surface. As the flow becomes more active over a wider region with heat gain, it increases the importance of buoyancy. Eventually, the flow becomes oscillatory as a result of interaction between buoyancy and thermocapillarity. The numerical simulations of oscillations show that the flow remains steady below a certain Ma, independent of Bi^*, and that Ma_{cr} depends slightly on Bi^* above this minimum Ma. Experimentally, when we increase T_H stepwise, we tend to reach this minimum Ma first so that the flow becomes oscillatory at this Ma regardless of T_R. In the case of concave liquid bridges, the onset of oscillations is much less affected by the free surface heat transfer, whether it is gain or loss.

Acknowledgements

This work is performed as a part of the Project Research on Marangoni Convection of JAXA. The financial support for the work performed at Case Western Reserve University was given by NASDA (National Space Development Agency of Japan) before it became JAXA and is gratefully acknowledged.

References

[1] F. Preisser, D. Schwabe, A. Scharmann, Steady and oscillatory thermocapillary convection in liquid columns with free cylindrical surface, J. Fluid Mech. 126 (1983) 545–567.

[2] H.C. Kuhlmann, H.J. Rath, Hydrodynamic instabilities in cylindrical thermocapillary liquid bridges, J. Fluid Mech. 247 (1993) 247–274.
[3] J. Masud, Y. Kamotani, S. Ostrach, Oscillatory thermocapillary flow in cylindrical columns of high Prandtl fluids, J. Thermophys. Heat Transfer 11 (1) (1997) 105–111.
[4] W.R. Hu, J.Z. Shu, R. Zhou, Z.M. Tang, Influence of liquid bridge volume on the onset of oscillation in floating zone convection: 1. experiments, J. Cryst. Growth 142 (3/4) (1994) 379–384.
[5] M. Wanschura, H.C. Kuhlmann, H.J. Rath, Linear stability of two-dimensional combined buoyant-thermocapillary flow in cylindrical liquid bridges, Phys. Rev. E 55 (6) (1997) 7036–7042.
[6] R. Monti, C. Albanese, L. Cartenuto, D. Castagnaolo, G. Evangelista, An investigation on the onset of oscillatory Marangoni flow, Adv. Space Res. 16 (7) (1995) 87–94.
[7] Y. Kamotani, L. Wang, S. Hatta, R. Selver, S. Yoda, Effect of free surface heat transfer on onset of oscillatory thermocapillary flow of high Prandtl fluid, J. Jpn. Soc. Microgravity Appl. 18 (2001) 283–288.
[8] Y. Kamotani, L. Wang, S. Hatta, A. Wang, S. Yoda, Free surface heat loss effect on oscillatory thermocapillary flow in liquid bridges of high Prandtl number fluids, Int. J. Heat Mass Transfer 46 (2003) 3211–3220.
[9] V.M. Shevtsova, M. Aliaksandr, M. Mohamed, A study of heat transfer in liquid bridges near onset of instability, J. Non-Equilib. Thermodyn. 30 (2005) 261–281.
[10] D. Castagnolo, L. Carotenuto, Numerical simulation of three-dimensional thermocapillary flows in liquid bridges, Numer. Heat Transfer Part A 36 (1999) 859–877.
[11] J. Leypoldt, H.C. Kuhlmann, H.J. Rath, Three-dimensional numerical simulation of thermocapillary flows in cylindrical liquid bridges, J. Fluid Mech. 414 (2000) 285–314.
[12] N. Imaishi, S. Yasuhiro, Y. Akiyama, S. Yoda, Numerical simulation of oscillatory Marangoni flow in half-zone liquid bridge of low Prandtl number, J. Cryst. Growth 230 (2001) 164–171.
[13] M. Lappa, Fluids, Materials & Microgravity: Numerical Techniques and Insights into Physics, Elsevier, 2004.
[14] B.-C. Sim, A. Zebib, Thermocapillary convection in cylindrical liquid bridges and annuli, C. R. Mech. 332 (2004) 474–486.
[15] A. Wang, Effects of free surface heat transfer and shape on thermocapillary flow of high Prandtl fluids, PhD Thesis, Case Western Reserve University, Cleveland, OH, 2005.
[16] J.H. Lee, A study of oscillatory thermocapillary flow in circular containers with CO_2 laser heating, PhD Thesis, Case Western Reserve University, Cleveland, OH, 1994.
[17] S.V. Patankar, Numerical Heat Transfer and Fluid Flow, Hemisphere, Washington, DC, 1980.
[18] A. Pline, Surface temperature measurements for the surface tension driven convection experiment, Technical Report, NASA TM101353, 1988.
[19] Y. Kamotani, J. Platt, Effects of free surface shape on combined thermocapillary and natural convection, J. Thermophys. Heat Transfer 6 (1992) 721–726.
[20] Y. Kamotani, S. Ostrach, Theoretical analysis of thermocapillary flow in cylindrical columns of high Prandtl number fluids, J. Heat Transfer 120 (1998) 758–764.